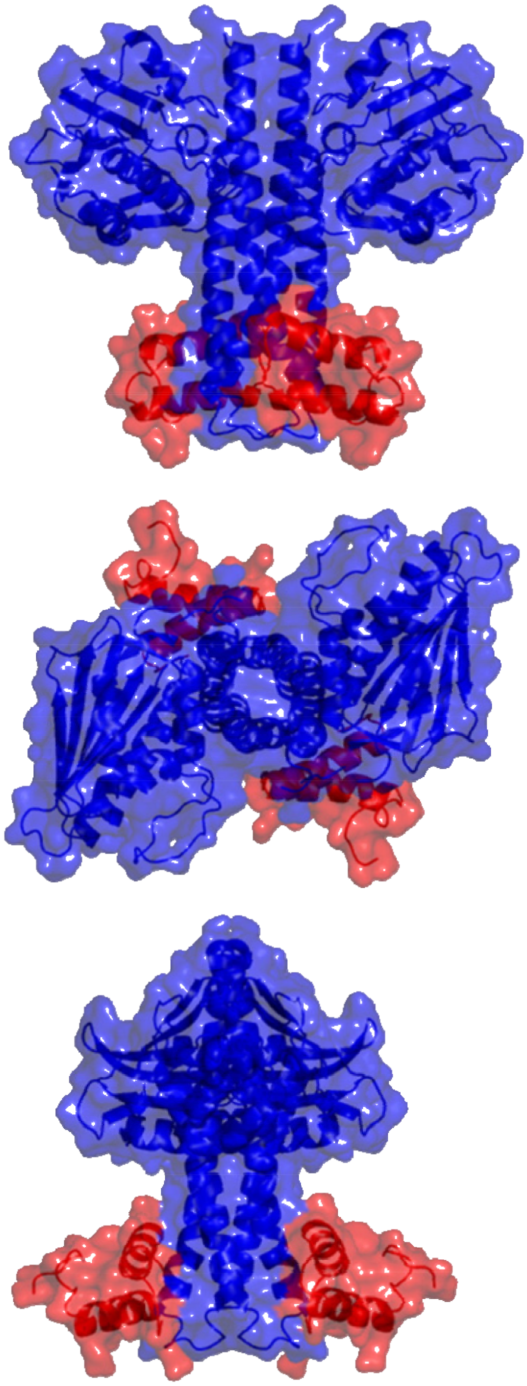

Supplementary Figure 1 The $KinA_2$-2Sda structure used as test case. The KinA molecules are coloured blue, while the Sda molecules are coloured red.

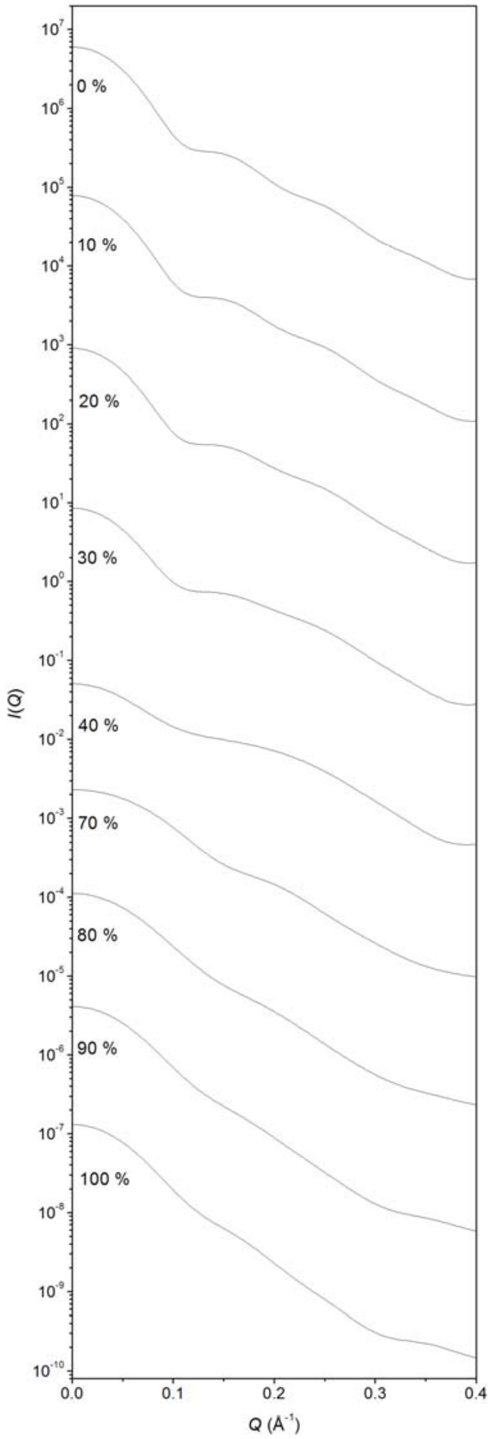

Supplementary Figure 2 Theoretical neutron scattering profiles generated from the KinA$_2$-2Sda complex (Supplementary Figure 1). The 0% ^2H_2O profile has units of 10^{-24} cm^2, with each subsequent profile off-set by a factor of 50^{-n} ($n_{10\%} = 1$, $n_{20\%} = 2$, $n_{30\%} = 3$, $n_{40\%} = 4$, $n_{70\%} = 5$, $n_{80\%} = 6$, $n_{90\%} = 7$, $n_{100\%} = 8$).

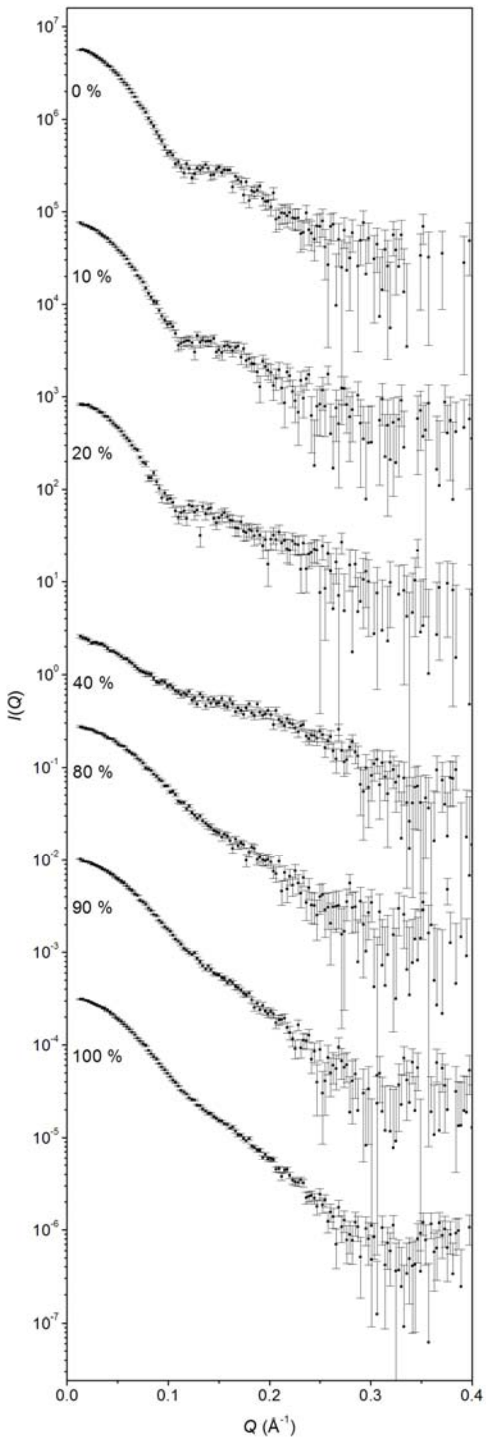

Supplementary Figure 3 Theoretical neutron scattering profiles generated from the $KinA_2$-2Sda complex (Supplementary Figure 1), with normally distributed noise applied to the data, with a level approximately equal to experimental data collected at ~12 mg/mL. The 0% ^2H_2O profile has units of 10^{-24} cm^2, with each subsequent profile off-set by a factor of 50^{-n} ($n_{10\%} = 1$, $n_{20\%} = 2$, $n_{40\%} = 3$, $n_{80\%} = 4$, $n_{90\%} = 5$, $n_{100\%} = 6$).

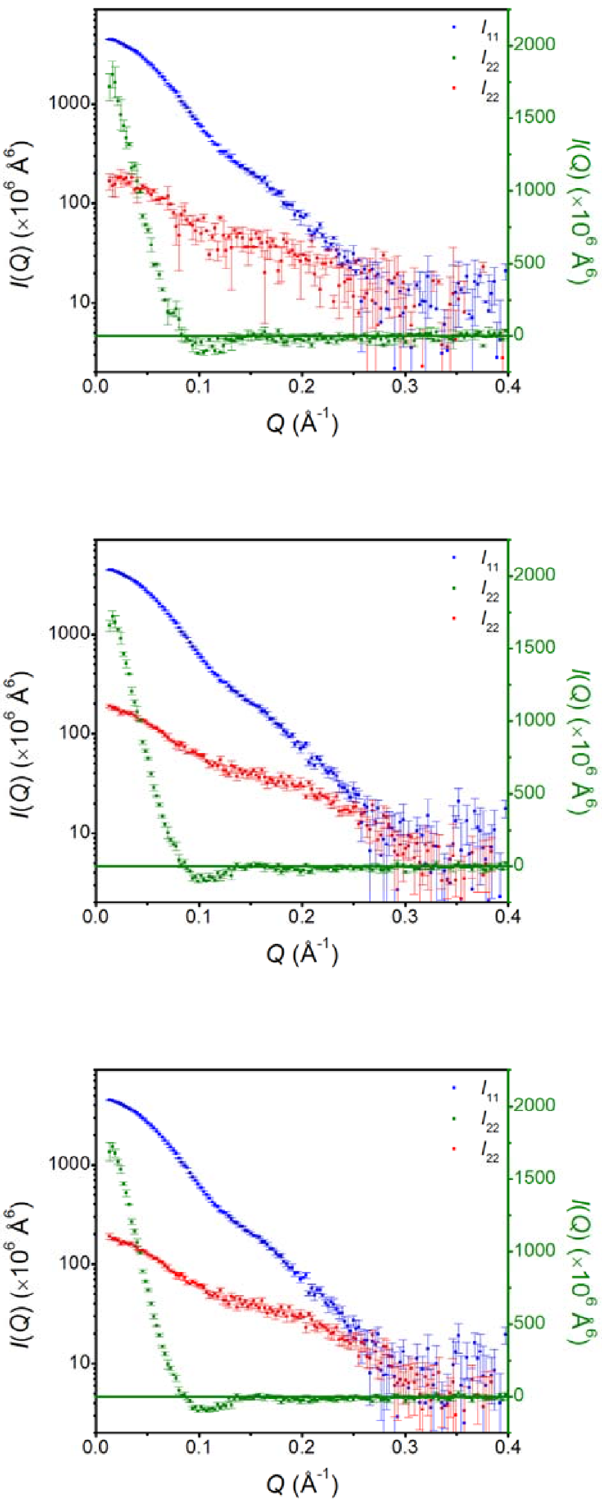

Supplementary Figure 4 Composite scattering functions using the scattering profiles shown in Supplementary Figure 3; **Top** Four contrast points (0%, 20%, 80%, 100%); **Middle** Five contrast points (0%, 20%, 40%, 80%, 100%); **Bottom** Seven contrast points (0%, 10%, 20%, 40%, 80%, 90%, 100%).

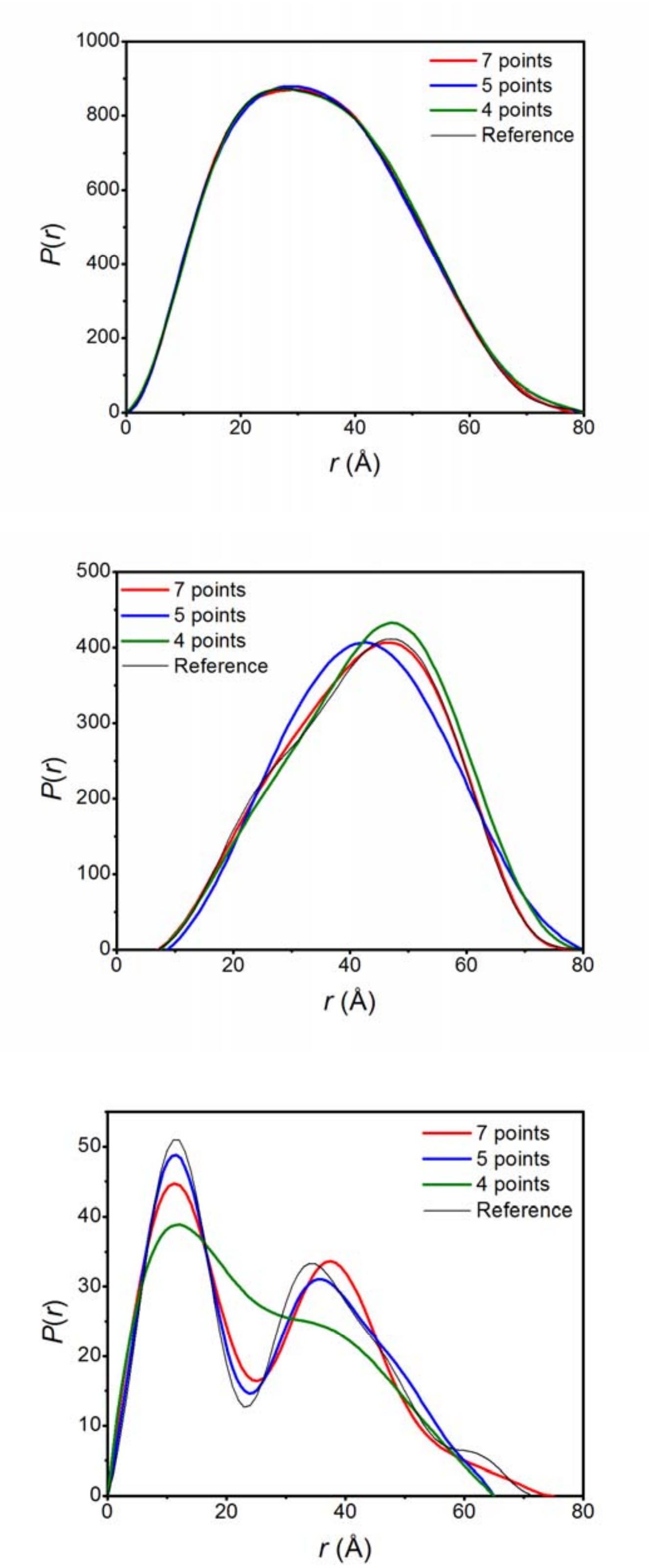

Supplementary Figure 5 $P(r)$ functions derived from the composite scattering functions (Supplementary Figure 4); **Top** I_{HH}; **Middle** I_{HD}; **Bottom** I_{DD}.

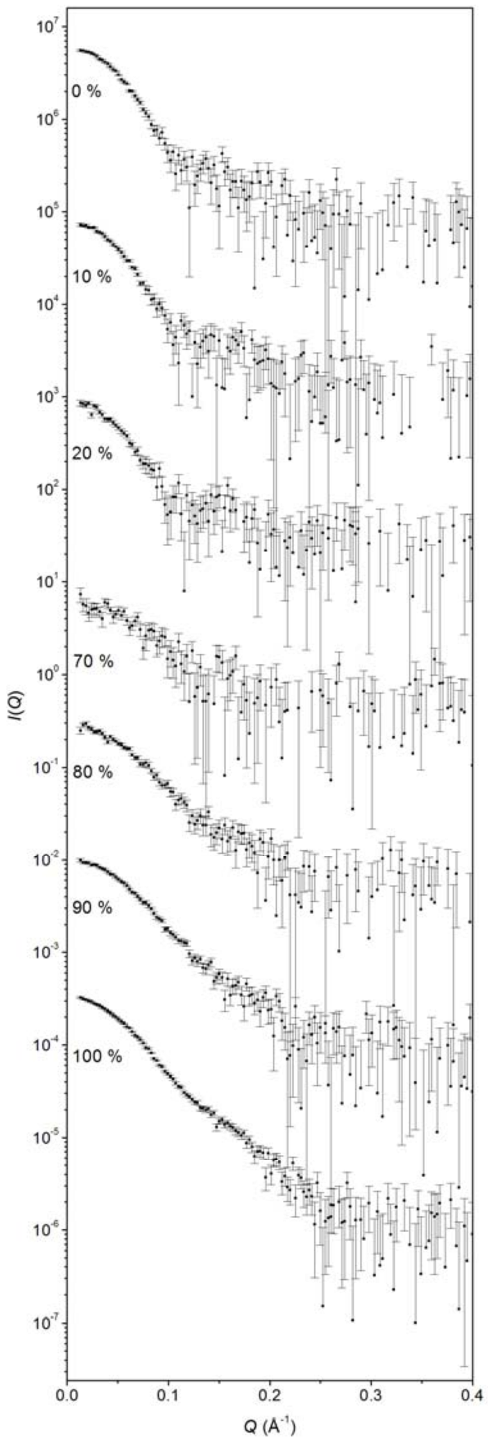

Supplementary Figure 6 Theoretical neutron scattering profiles generated from the $KinA_2$-2Sda complex (Supplementary Figure 1), with normally distributed noise applied to the data, with a level approximately equal to experimental data collected at ~4 mg/mL. The 0% ^2H_2O profile has units of 10^{-24} cm^2, with each subsequent profile off-set by a factor of 50^{-n} ($n_{10\%} = 1$, $n_{20\%} = 2$, $n_{70\%} = 3$, $n_{80\%} = 4$, $n_{90\%} = 5$, $n_{100\%} = 6$).

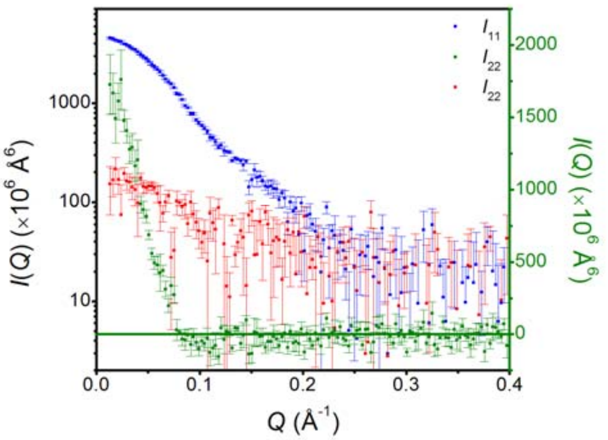

Supplementary Figure 7 Composite scattering functions using all the scattering profiles shown in Supplementary Figure 6 (0%, 10%, 20%, 40%, 80%, 90%, 100%). The effect of fewer contrast points is not test here, because the accuracy of the extraction is limited by the noise level in the data.

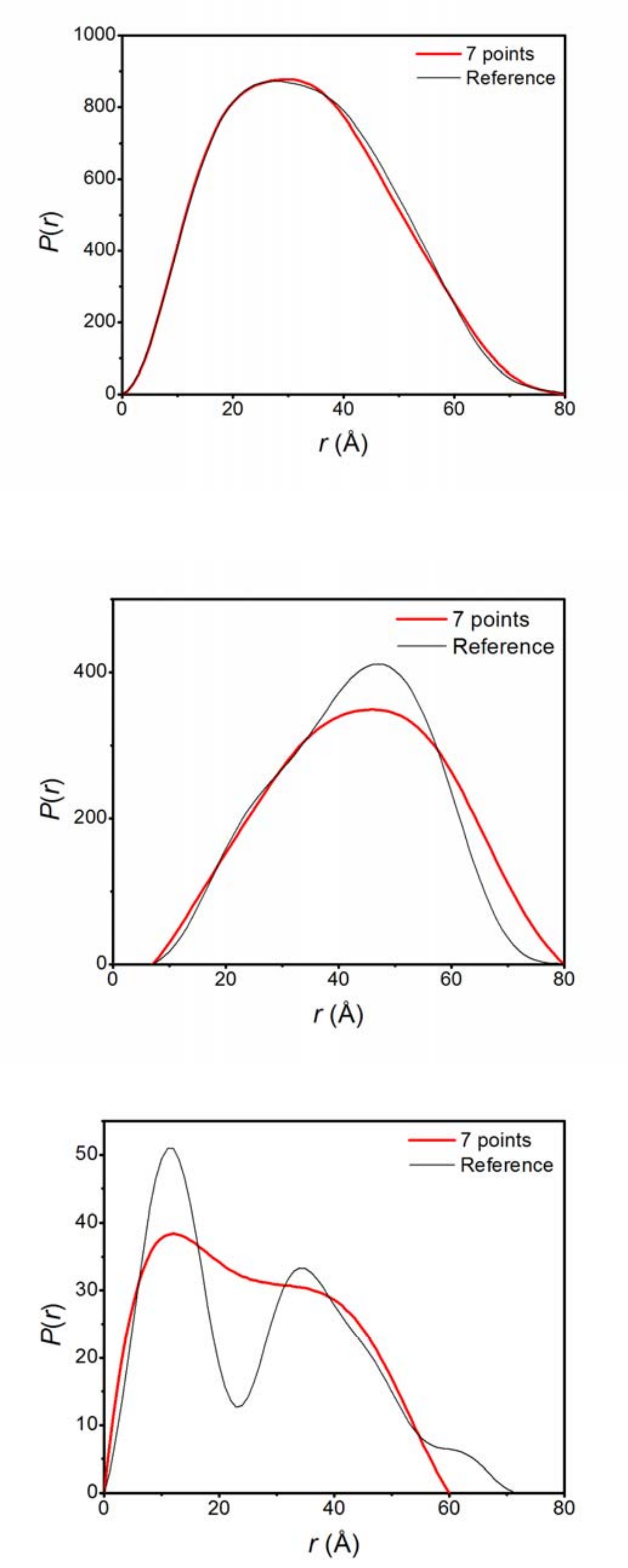

Supplementary Figure 8 $P(r)$ functions derived from the composite scattering functions (Supplementary Figure 7); **Top** I_{HH}; **Middle** I_{HD}; **Bottom** I_{DD}.

Supplementary Table 1 Comparison of the radii of gyration for the KinA:Sda complex obtained from various methods, using different combinations of contrast points.

	R_H (Å)	R_D (Å)	$D^{§}$ (Å)	R_m (Å)
Actual values†	25.74 - 26.88	20.54 - 21.37	29.37 – 32.30	27.54
Low Noise (4 contrast points)				
Parallel Axis	25.71(19)	18(5)	33(4)	-
Stuhrmann	-	-	-	27.53(27)
Extraction	25.52(27)	23.1 (12)	-	-
Low Noise (5 contrast points)				
Parallel Axis	25.64(6)	21.0(4)	31.0(7)	-
Stuhrmann	-	-	-	27.4(12)
Extraction	25.74(21)	22.6 (10)	-	-
Low Noise (7 contrast points)				
Parallel Axis	25.71(10)	21.0(5)	31.0(8)	-
Stuhrmann	-	-	-	27.50(15)
Extraction	25.64(20)	21.8 (12)	-	-
High Noise (7 contrast points)				
Parallel Axis	25.94(24)	17(7)	33(5)	-
Stuhrmann	-	-	-	33(5)
Extraction	25.90(25)	18 (4)	-	-

Implementation of composite scattering function extraction

The composite scattering functions are calculated via minimisation of a conventional weighted least-square residual:

$$\varepsilon'_q = \sum_i \left[\frac{I_{i,q}^{\exp} - A_i I_{11,q} - B_i I_{12,q} - C_i I_{22,q}}{\sigma(I_{i,q})} \right]^2 ,$$

where $A_i = \Delta\overline{\rho}_{1,i}^2$, $B_i = \Delta\overline{\rho}_{1,i}\Delta\overline{\rho}_{2,i}$ and $C_i = \Delta\overline{\rho}_{2,i}^2$, q distinguishes between each resolution bin, and the subscript i represents each contrast variation data set. A minimum occurs when the derivative of the residual with respect to each variable, V_j, is equal to zero,

$$\frac{\partial \varepsilon'_q}{\partial V_j} = 0 \,.$$

This leads to the set of linear equations

$$\begin{bmatrix} \sum_i \frac{I_{i,q}^{\exp} A_i}{\sigma^2(I_{i,q})} \\ \sum_i \frac{I_{i,q}^{\exp} B_i}{\sigma^2(I_{i,q})} \\ \sum_i \frac{I_{i,q}^{\exp} C_i}{\sigma^2(I_{i,q})} \end{bmatrix} = \begin{bmatrix} \sum_i \frac{A_i^2}{\sigma^2(I_{i,q})} & \sum_i \frac{A_i B_i}{\sigma^2(I_{i,q})} & \sum_i \frac{A_i C_i}{\sigma^2(I_{i,q})} \\ \sum_i \frac{B_i A_i}{\sigma^2(I_{i,q})} & \sum_i \frac{B_i^2}{\sigma^2(I_{i,q})} & \sum_i \frac{B_i C_i}{\sigma^2(I_{i,q})} \\ \sum_i \frac{C_i A_i}{\sigma^2(I_{i,q})} & \sum_i \frac{C_i B_i}{\sigma^2(I_{i,q})} & \sum_i \frac{C_i^2}{\sigma^2(I_{i,q})} \end{bmatrix} \begin{bmatrix} I_{11,q} \\ I_{12,q} \\ I_{22,q} \end{bmatrix}$$

which can be expressed in the form

$$\mathbf{X}_q = \mathbf{P}_q \mathbf{I}_q \,.$$

This can be rearranged to give the composite scattering functions $\mathbf{I}_q$,

$$\mathbf{I}_q = \mathbf{P}_q^{-1} \mathbf{X}_q \,.$$

The variance for each data point q, for each composite scattering function is then calculated via

$$\sigma^2(I_{k,q}) = \frac{\varepsilon_q}{N-3} P^{-1}_{kk,q} = \chi^2_q P^{-1}_{kk,q} \cdot$$

Implementation of the parallel-axis theorem

Parameters for the parallel-axis theorem are solved via minimisation of the least-squares residual

$$\varepsilon = \sum_i \left[\frac{R^2_{i,obs} - f'_{i,1} R_1^2 - f'_{i,2} R_2^2 - f'_{i,1} f'_{i,2} D^2}{\sigma^2\left(R^2_{i,obs}\right)} \right]^2 .$$

Again a minimum occurs when the derivative of the residual with respect to each variable, V_j, is equal to zero. A corresponding set of linear equations are solved, and the variances determined in an analogous fashion to the composite scattering functions.

Implementation of the Stuhrmann analysis

Parameters for the Stuhrmann plot are solved via minimisation of the least-squares residual

$$\varepsilon = \sum_i \left[\frac{R^2_{i,obs} - R^2_m - \frac{\alpha}{\Delta\overline{\rho}_i} + \frac{\beta}{\Delta\overline{\rho}_i^2}}{\sigma^2\left(R^2_{i,obs}\right)} \right]^2$$

Again a minimum occurs when the derivative of the residual with respect to each variable, V_j, is equal to zero. A corresponding set of linear equations are solved, and the variances determined in an analogous fashion to the previous two examples.